UDC 622.267.5 DOI: https://doi.org/10.15407/geotm2024.168.139

THE INFLUENCE OF THE FEATURES OF OUTBURST-PRONE ROCKS POSITION IN THE FLOOR OF THE STOPE ON STRESS FIELDS AND DEGASATION PROCESS

[1]Krukovska V., [1]Krukovskyi O., [2]Yanzhula O., [1]Kostrytsia A., [1]Kocherga V.

[1]M.S. Poliakov Institute of Geotechnical Mechanics of the National Academy of Sciences of Ukraine
[2]Coal Directorate METINVEST HOLDING LLC

Abstract. Rock-gas outbursts happen when mine workings are driven near low-permeability sandstones, which contain gas under high pressure, and most of such outbursts are triggered by shot firing. In particular, when sections of the powered support are clamped in the stope, it is necessary to explode the rock under them, which is dangerous if the outburst-prone sandstone is located in the floor of the stope. One of the factors causing the rock-gas outburst is a certain combination of the stress-dependent permeability of the sandstone and the near-floor rock and gas pressure. Therefore, the purpose of the work is to study the change in the stress state of the host rocks and gas filtration process in the outburst-prone sandstone located in the floor of the stope, with different composition of the near-floor rocks. To achieve the goal, methods of numerical simulation of time-dependent processes of elastic-plastic deformation and gas filtration were used. A stope with sections of the powered support was considered, in the floor of which siltstone and outburst-prone sandstone are located. The computations were performed with variations in the thickness and strength of the siltstone bed above the sandstone.

It is shown that the values of the maximum and minimum components of the principal stress tensor gradually decrease in the floor of the stope, the sandstone is unloaded from the rock pressure. This leads to an increase in its permeability, the start of the methane filtration and degasation process. The composition of near-contour rocks greatly affects the distribution of geomechanical and filtration parameters. In the presence of the siltstone bed with a certain strength, a not unloaded bridge with lower permeability appears above the sandstone, and its degasation slows down significantly. If the thickness of the siltstone bed increases, the width of this bridge also increases, and methane filtration in the floor of the stope stops. In this case it is an obstacle that delays or completely prevents the degassing of gas-bearing rocks that lie below.

The results of the above analyses should aid evaluation of potential measures to prevent the rock-gas outburst during blasting operations for the movement of sections of powered support in the stope. A better understanding of this problem could save considerable time and expense for future technological operations in similar mining conditions.

Keywords: rock-gas outburst, rock deformation, coupled processes, stope, gas filtration, numerical simulation.

1. Introduction

Most reported outbursts at coal mines occur from the coal face. However, gas-dynamic phenomena often occur from outburst-prone host rocks [1, 2], and their prediction and prevention are one of the major challenges to the rock mechanics and rock engineering community [3, 4].

Rock-gas outbursts happen during underground mining when mine workings are driven near low-permeability sandstones, which contain gas under high pressure [1, 5] and most of such outbursts are triggered by shot firing [2]. A siltstone bed often interlay between the sandstone and the coal seam. When a siltstone bed intervenes between the mine working and the outburst-prone sandstone, this siltstone must fail prior to the initiation of outburst from the sandstone [6]. The stopes of the southern panel of 10th block in PJSC Colliery Group "Pokrovske" are in precisely such mining and geological conditions [7, 8]. In this area, the siltstone of medium strength, with a thickness of 0–2.5 m, and the strong, outburst-prone sandstone with a thickness of 2.5–19 m are located in the coal seam floor. If sections of the powered support are clamped between the seam floor and the overhanging rock console in stopes of 10th block, it is necessary to explode the rock under them, which is dangerous near the outburst-prone sandstone.

Scientists in different countries have studied outburst-prone sandstones [1–4, 9, 10], their structural transformations in the process of catagenesis [11], permeability, porosity, moisture and acoustic properties [1, 12, 13], behaviour during destruction, patterns of the crack propagation and the ejection of rock fragments on the unloading surface [14], the mechanism of occurrence and course of rock-gas outburst [9, 15, 16]. A rock-gas outburst is a complex dynamic phenomenon, which is determined by many factors, including stresses in the rocks caused by the weight of rock mass and mining operations, gas pressure, physical-mechanical and filtration properties of the rocks [2–4, 16, 17]. Mining excavation releases strain energy of the host rock. Gas emission can release not only gas expansion energy but also strain energy of the host rock [3], as evidenced by many measured results, which show that with gas emission, the rock permeability coefficients increase markedly [18]. And the speed of these processes determines the possibility of a gas-dynamic phenomenon.

Outbursts, regardless of the environment in which they occur, have a common mechanism and are a self-regulated process that occurs in a rather narrow range of dynamic parameters values [16]. Therefore, a thorough study of the dynamic processes of host rocks deformation and gas filtration, which occur directly in the outburst-prone zone, is necessary in order to determine the potential outburst hazard.

In this regard, the purpose of this work is to study the change in the stress state of the host rocks and gas filtration process in the outburst-prone sandstone located in the floor of the stope, with different composition of the near-floor rocks.

To achieve the goal, the following tasks were solved:

1) to perform a numerical simulation of the coupled processes of deformation of a rock mass with a stope and supporting elements and gas filtration from gas-bearing rocks located in the floor of the stope;

2) to investigate the influence of the composition of the near-floor rocks on the distribution of stresses and gas filtration process;

3) to investigate the influence of the strength of the rock layer above the outburst-prone sandstone on the distribution of stresses and gas filtration process in the floor of the stope.

2. Methods

To solve the problem, a numerical simulation of the coupled processes of elastic-plastic rock deformation and gas filtration was performed [19, 20]. The Coulomb-Mohr failure criterion was used to describe the failure behaviour of the rocks [21, 22]. The permeability k of rocks, depending on their stress state, was determined by the equations obtained by the authors earlier [7, 23, 24]. The problem was solved using the finite element method [25–27] with the help of authors' software. At each time step, the stress field, inelastic deformation zones, the stress-dependent field of permeability coefficients, gas pressure and gas filtration rate were calculated. At the next time step, when calculating the stress field, the change in gas pressure in the crack-pore space of the rock was taken into account.

The stress field was analysed using geomechanical parameters Q^*, which characterizes the difference of the stress tensor components, P^*, which characterizes unloading of rocks from rock pressure, and R^*, which defines zones of increased rock pressure:

$$Q^* = \frac{\sigma_1 - \sigma_3}{\gamma H}; \quad P^* = \frac{\sigma_3}{\gamma H}; \quad R^* = \frac{\sigma_1}{\gamma H},$$

where σ_1, σ_3 – maximum and minimum components of the principal stress tensor, Pa; γ – the averaged weight of the overlying mine rocks, N/m^3; H – the mining depth, m.

A longitudinal section of a 2-m-high stope with the powered support was considered, figure 1 shows the central fragment of the finite element mesh for this problem. Also figure 1 shows the location of the rock blasting hole under the powered support when it is clamped.

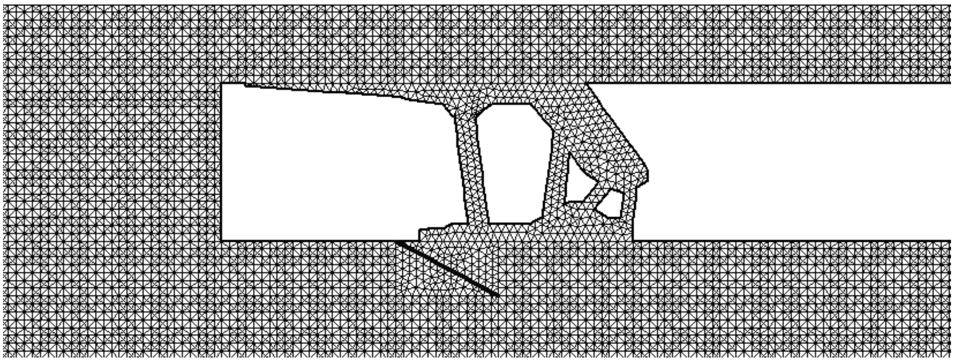

Figure 1 – The central fragment of the finite element mesh

Determination of the properties of outburst-prone sandstones proved that they can differ significantly in terms of compressive strength and modulus of elasticity, table 1. But their tensile strength is limited to the range of 3-7 MPa, porosity is in the range of 3-11%, the in situ permeability is generally less than 0.02 mD [1].

Table 1 – Properties of outburst-prone sandstones

Location of the outburst-prone sandstone	Strengths		Elastic properties E, GPa	Porosity, %	Perm k, mD
	σ_c, MPa	σ_t, MPa			
Sydney Coalfield, Nova Scotia, Canada [1]	100-170	-	8-10	3	0.005-0.04
26 Colliery, Glace Bay, Nova Scotia, Canada [2]	76.3	5.8	18.5	5.24	0.03
Haishiwan Colliery, Lanzhou, Gansu Province, China [3]	32	2.6	33.5	7	-
Yongrong mining area, China [9]	58.5	4.13	-	4.49	-
Yongchuan Coal Mine, China [10]	62.77	7.48	27.3	4.49	-
O.O. Skochinsky Mine [28], Ukraine	-	-	-	7.5	0.07
PJSC Colliery Group "Pokrovske", Ukraine	38-86	4-6	-	5-11.5	-

When performing the calculations, it was assumed that the properties of the outburst-prone sandstone in the floor of the mine correspond to the conditions of the southern panel of 10th block in PJSC Colliery Group "Pokrovske", table 1. Missing mechanical and filtration characteristics are taken as average according to the table. 1. It was also accepted that the mining depth is 1200 m. The composition of the rocks in the coal seam floor varied according to the table 2.

Table 2 – Composition of the rocks in the coal seam floor

Rocks	Ultimate strength σ_c, MPa	Thickness *m*, m
Sandstone	45.1	15
Siltstone	20.8	3
Coal	17.3	2.0
Siltstone	20.8	0.0
	10.4; 15.6; 20.8; 31.2	0.5
	20.8	1.0
	20.8	3.0
Sandstone	45.1	10

The natural gas content in the coal seam in the 10th block of PJSC Colliery Group "Pokrovske" is 18 m^3/t, in the sandstone it is 2 m^3/t. Information on the in situ gas pressure in the sandstone is very sparse. Gas pressures were measured at 6 MPa in the sandstone of 26 Colliery (Glace Bay, Nova Scotia, Canada) at a depth of 780 m [2]. A reservoir engineering "rule of thumb" estimates pressures in accordance with the hydrostatic head of water $\gamma_w H$ [2] or as $0.8\gamma_w H$ [29]. According to the above considerations, the most probable gas pressure at a depth of 1200 m is in the range of 9.2-12.0 MPa. In further calculations, it was assumed that the gas pressure in the outburst-prone sandstone is 9 MPa.

The duration of one time step *i* is 2.7 hours.

3. The influence of the composition of the near-floor rocks in the stope on the distribution of stresses and gas filtration process

Alternation of layers "sandstone-siltstone-coal-siltstone-sandstone" is one of the most common types of occurrence of coal-bearing rocks.

We will consider four cases: when there is no siltstone bed in the floor of the stope above sandstone with a thickness of m = 10 m and a strength of σ_c = 45.1 MPa; when the thickness m_{sil} of the siltstone (σ_c = 20.8 MPa) is 0.5 m, 1.0 m and 3.0 m; and we will analyse the influence of such rock composition on the course of deformation and filtration processes in the host rocks. Figure 2 shows the results of stress field calculations in the studied area at time step i = 10; Figure 3 shows the graphs of changes in geomechanical parameters in the floor of the stope, along a vertical line passing 0.2 m before the point of drilling the hole.

In all cases (figure 2a), a zone of abutment pressure begins to form at the mine face, where the maximum component of the principal stress tensor coincides with the vertical stresses [8]. Zones where $R^* > 1.2$ spread from the upper and lower corners of the stope, figure 2a, which will close in a semi-ring in a day.

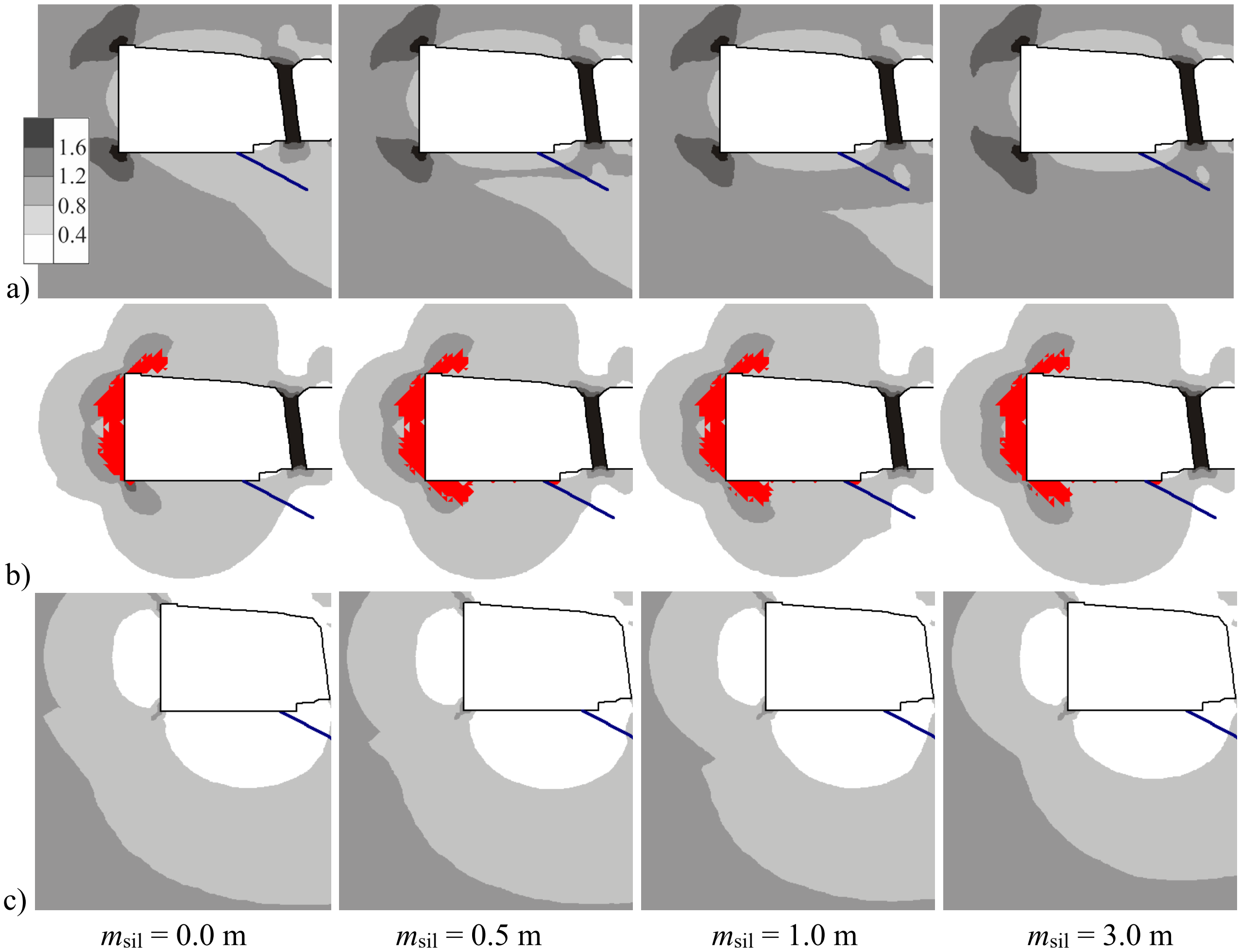

a) R^* parameter; b) Q^* parameter and zones of inelastic deformations (red colour); c) P^* parameter

Figure 2 – Distribution of geomechanical parameters in the host rocks around the stope with powered support in cases when there is no siltstone bed in the floor of the stope; the siltstone bed thickness is m_{sil} = 0.5 m; 1.0 m and 3.0 m

In the floor of the stope, where the maximum stresses act in the horizontal direction [8], R^* parameter values gradually decrease, the sandstone is unloaded from the rock pressure (figure 2a, first from the left). This leads to an increase in its permeability, which increases the intensity of the methane filtration process from the unloaded area into the mine atmosphere. The outburst-prone sandstone is gradually degassed, and, as it is known, this reduces its outburst hazard.

The composition of the rocks greatly affects the distribution of R^* parameter values, figure 2a, which is also clearly visible on the graph, figure 3a. The region with small R^* parameter values ($0.4 < R^* < 0.8$) in the rocks of the floor of the stope has the largest area in the case when there is no siltstone above the sandstone, figure 2a. The decrease of stress in sandstone is larger than in siltstone under the same unloading strain because the modulus of elasticity of sandstone, as well as its bulk modulus, is higher [3]. Under the condition of m_{sil} = 0.5 m, an unloaded bridge with lower permeability appears in siltstone at the contact with sandstone, where $0.8 < R^* < 1.2$. At m_{sil} = 1.0 m, the width of this bridge increases from 0.2 m to 0.8 m (figure 3a), and at m_{sil} = 3.0 m, the unloaded zone in the floor of the stope disappears.

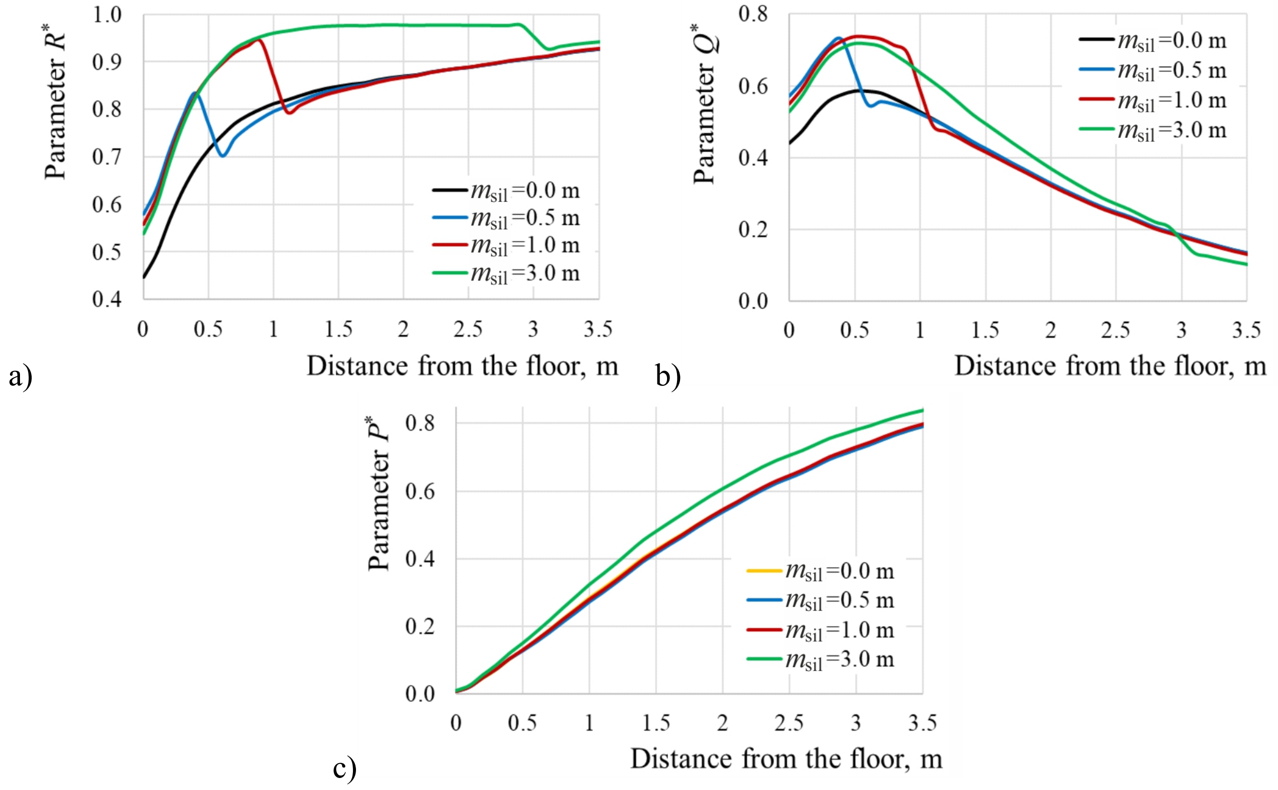

a) R^* parameter; b) Q^* parameter; c) P^* parameter

Figure 3 – Graphs of changes in geomechanical parameters in the floor of the stope when varying the siltstone bed thickness

The zone of inelastic deformations at the mine face, in the coal seam, is formed in all four cases, but it is absent in the floor of the stope, when much stronger sandstone lies directly under the coal seam (figure 2b, first from the left). It is obvious that Q^* parameter values in the floor of the stope also depends very much on the composition of the rocks, figure 3b, due to the component $\sigma_1/\gamma H$.

The value of the P^* parameter in the studied part of the floor of the stope changes slightly (figures 2c and 3c). If the unloading of overworked rocks is characterized by P^* parameter, then it can be assumed that the composition of the rocks has almost no effect on this process.

Now let's investigate how the process of methane filtration from the gas-bearing sandstone into the mine atmosphere takes place in the four considered cases. The field of permeability coefficients, calculated from the parameters of the stress state, methane pressure, and directions of its filtration at the moment of time $i = 10$, are shown in figure 4, graphs of changes in filtration parameters are shown in figure 5. It can be seen that in each case, a gas-permeable filtration area is formed around the stope, figure 4a. In the first three figures of this series, the sandstone is visible, which is shown in light grey colour because its initial, natural permeability, accepted in the calculations, is 0.025 mD.

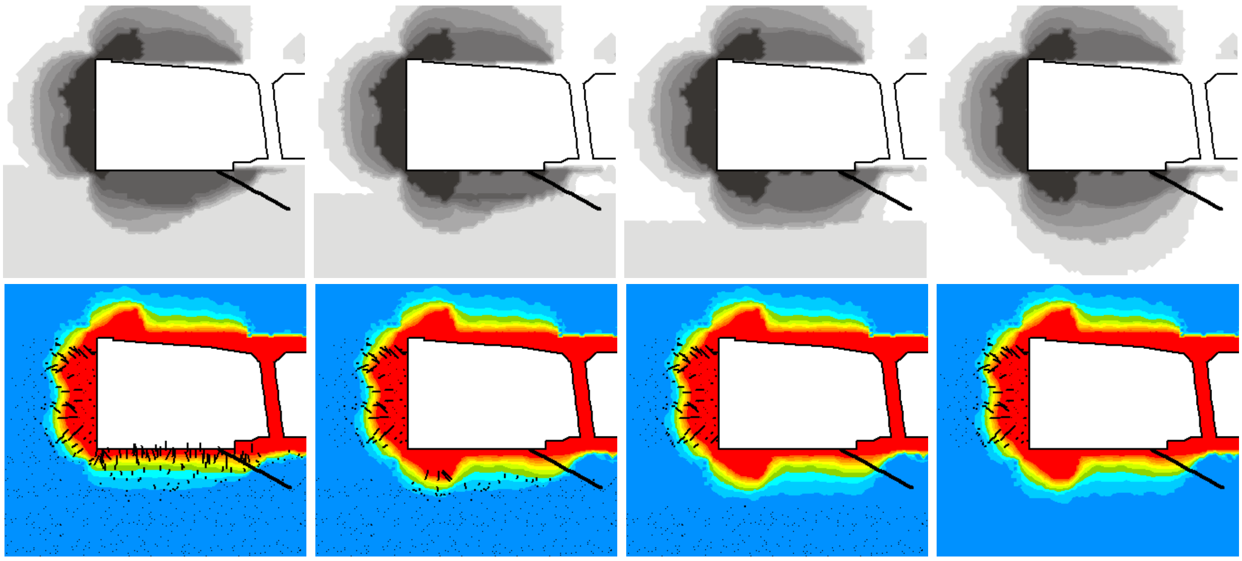

a)

b)

m_{sil} = 0.0 m m_{sil} = 0.5 m m_{sil} = 1.0 m m_{sil} = 3.0 m

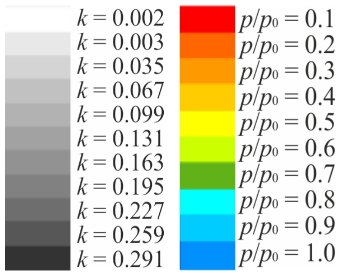

a) permeability k; b) relative gas pressure p/p_0 and directions of gas filtration.

Figure 4 – Distribution of filtration parameters in the host rocks around the stope with powered support in cases when there is no siltstone bed in the floor of the stope; the siltstone bed thickness is m_{sil} = 0.5 m; 1.0 m and 3.0 m

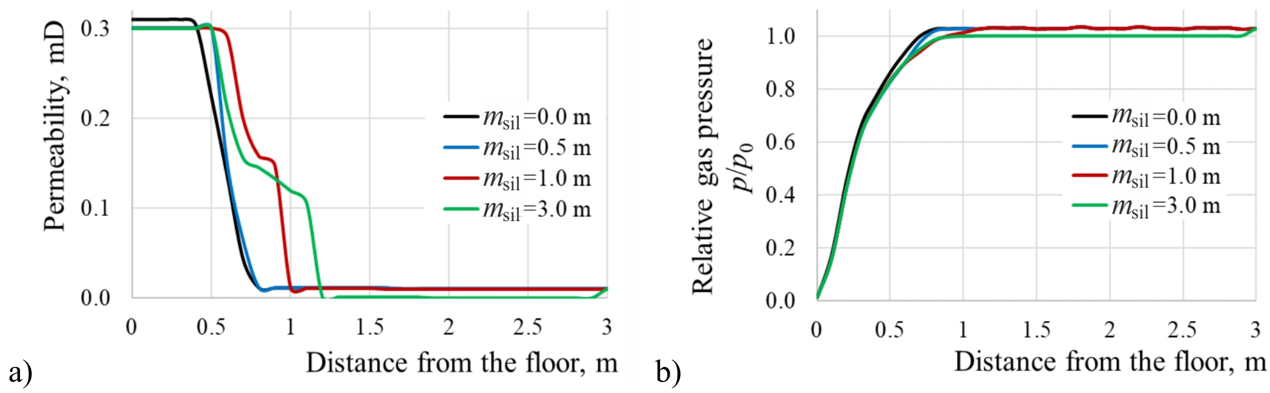

a) permeability k; b) relative gas pressure p/p_0

Figure 5 – Graphs of changes in filtration parameters in the floor of the stope when varying the siltstone bed thickness

Within the filtration area, the gas pressure drops (figure 4b, m_{sil} = 0.0 m, 5b), methane moves from the coal seam and sandstone in the floor of the stope, where it is under high pressure, into the mine atmosphere, where the air pressure is much lower and equal to atmospheric pressure. Black strokes in figure 4b show the directions of gas filtration from the sources of its emission. Based on their number and length, which is proportional to the modulus of the gas filtration rate, it is possible to draw a conclusion about the high intensity of the sandstone degasation process in the case when there is no siltstone bed in the floor of the stope. If a half-meter siltstone bed is located above the sandstone, degassing of the sandstone slows down significantly. In the case of an increase in the siltstone bed thickness, methane filtration in the floor of the stope stops until the permeable area spreads to the gas-bearing sandstone. At the time step $i = 10$, gas filtration from the sandstone does not occur (figure 4b, cases $m_{sil} = 1.0$ m and $m_{sil} = 3.0$ m).

4. The influence of the strength of the rock layer above the outburst-prone sandstone on the distribution of stresses and gas filtration process

Let's analyse how deformation and filtration processes in the floor of the stope with outburst-prone sandstone is affected by the strength of the siltstone located above it.

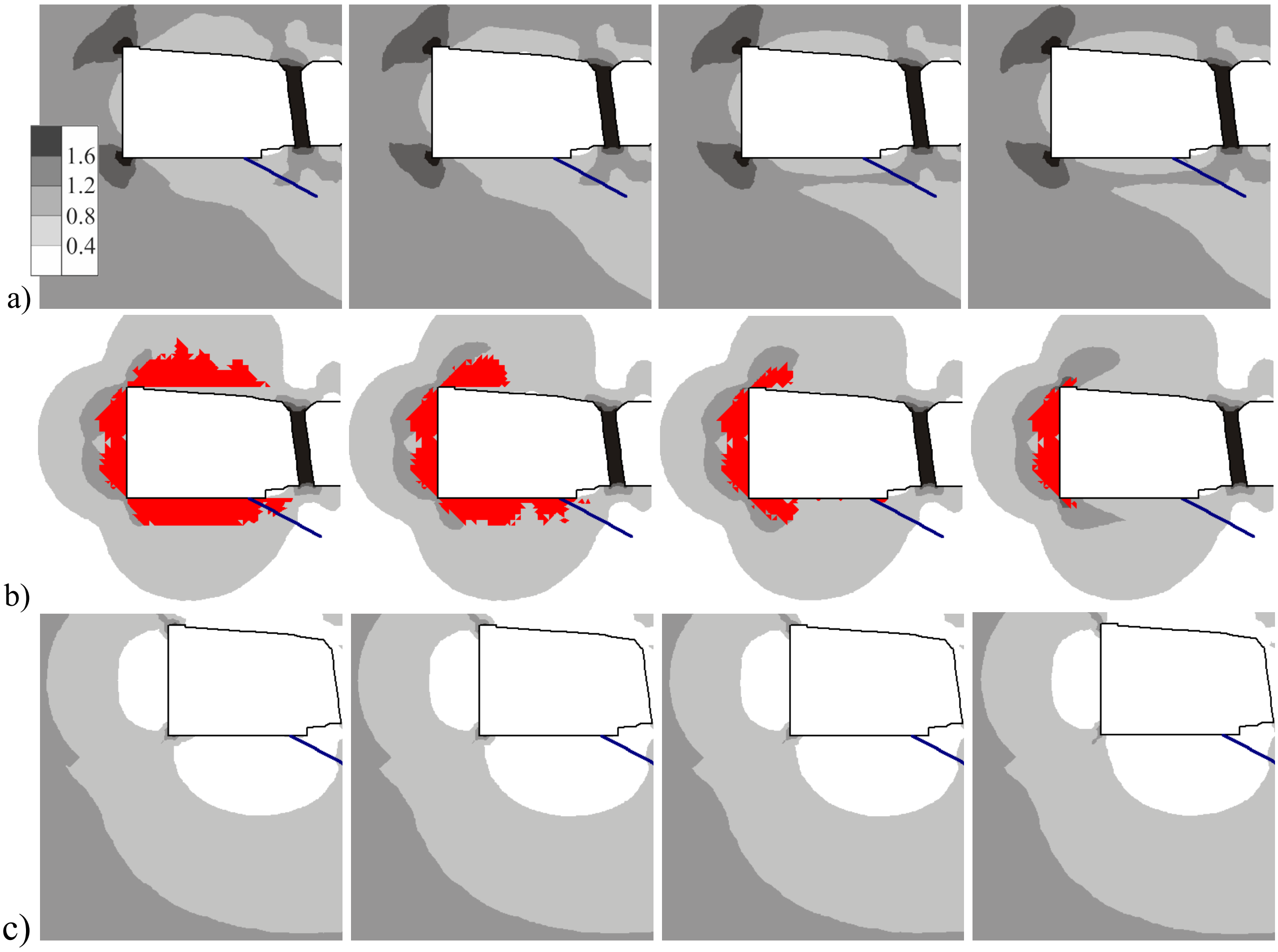

$\sigma_c = 10.4$ MPa $\sigma_c = 15.6$ MPa $\sigma_c = 20.8$ MPa $\sigma_c = 31.2$ MPa

a) R^* parameter; b) Q^* parameter and zones of inelastic deformations (red colour); c) P^* parameter

Figure 6 – Distribution of geomechanical parameters in the host rocks around the stope with powered support in cases when the siltstone bed has a strength limit of $\sigma_c = 10.4$ MPa, 15.6 MPa, 20.8 MPa, and 31.2 MPa

We will consider four cases when the siltstone bed with a thickness of $m_{sil} = 0.5$ m has a strength limit of $\sigma_c = 10.4$ MPa, 15.6 MPa, 20.8 MPa, and 31.2 MPa. The results of stress field calculations in the studied area at the time step $i = 10$ are shown in figure 6, figure 7 shows the graphs of changes in geomechanical parameters in the floor of the stope, along a vertical line passing 0.2 m in front of the hole drilling point.

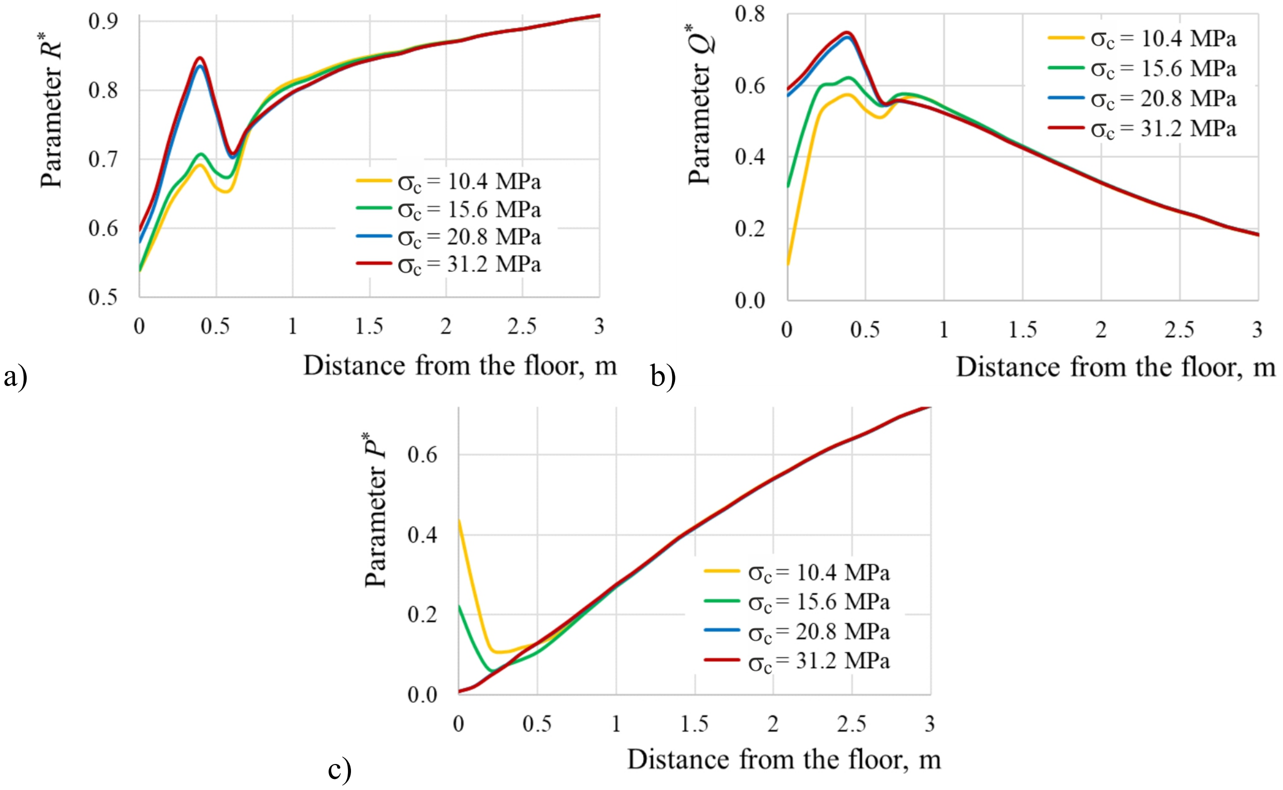

a) R^* parameter; b) Q^* parameter; c) P^* parameter

Figure 7 – Graphs of changes in geomechanical parameters in the floor of the stope when varying the siltstone's strength limit

If the weak siltstone bed lies above the hard sandstone, it is completely destroyed (figure 6b, $\sigma_c = 10.4$ MPa), the zone of inelastic deformations extends to the entire depth of 0.5 m. When the strength of the siltstone increases, the area of this zone decreases both in the floor and in roof of the stope. Under the condition $\sigma_c = 31.2$ MPa, the zone of inelastic deformations in siltstone practically disappears. The stressed state of the destroyed rocks approaches the state of bulk materials, while the maximum component of the principal stress tensor significantly decreases and the minimum component increases. Therefore, the values of the parameter R^* in the zone of inelastic deformations are low $0.4 < R^* < 0.8$ (figure 6a, $\sigma_c = 10.4$ MPa and $\sigma_c = 15.6$ MPa), and the values of the parameter P^*, on the contrary, are increased (figure 7c). This is clearly visible in graphs 7a and 7b, in the zone of inelastic deformations, at a distance of 0.0-0.5 m from the floor of the stope.

If the siltstone bed lying above the sandstone has a strength of σ_c = 20.8 MPa or σ_c = 31.2 MPa, it remains intact, and a not unloaded bridge, where 0.8 < R^* < 1.2, appears in it at the contact with the sandstone, figure 6a.

The values of permeability coefficients in the floor of the stope, in siltstones with lower strength (figures 8a and 9a, σ_c = 10.4 MPa and σ_c = 15.6 MPa) are very high, and therefore methane freely enters from the gas-bearing sandstone into the mine atmosphere. Methane pressure in this area drops rapidly (figure 9b); the number and length of strokes showing the directions of gas filtration from the sources of its release in figure 8b, testify to the high intensity of the sandstone degassing process.

a)

b)

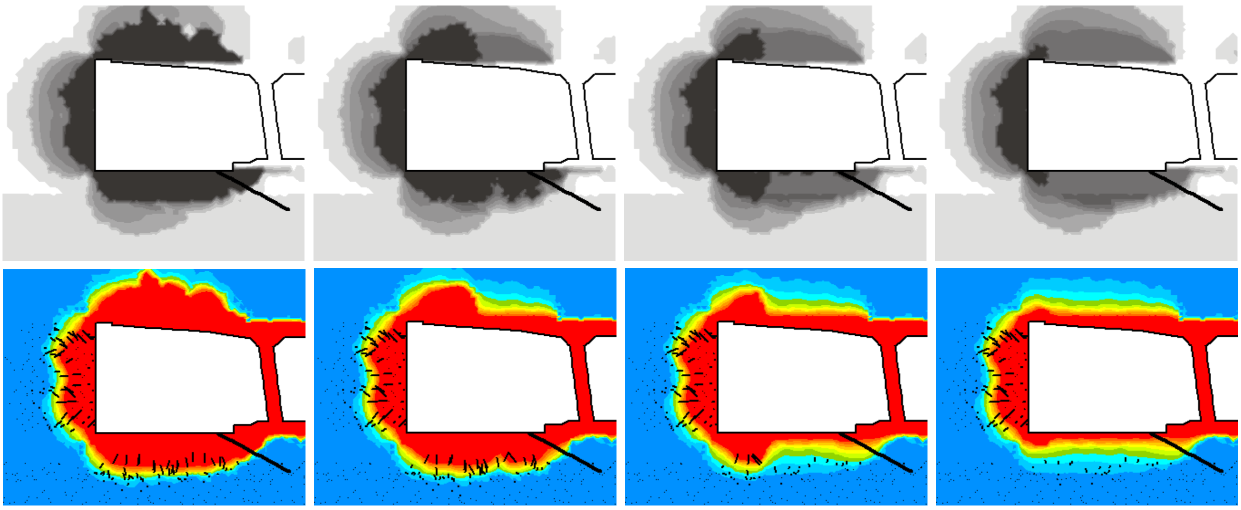

σ_c = 10.4 MPa σ_c = 15.6 MPa σ_c = 20.8 MPa σ_c = 31.2 MPa

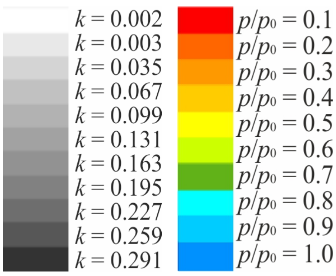

a) permeability k; b) relative gas pressure p/p_0 and directions of gas filtration

Figure 8 – Distribution of filtration parameters in the host rocks around the stope with powered support in cases when the siltstone bed has a strength limit of σ_c = 10.4 MPa, 15.6 MPa, 20.8 MPa, and 31.2 MPa

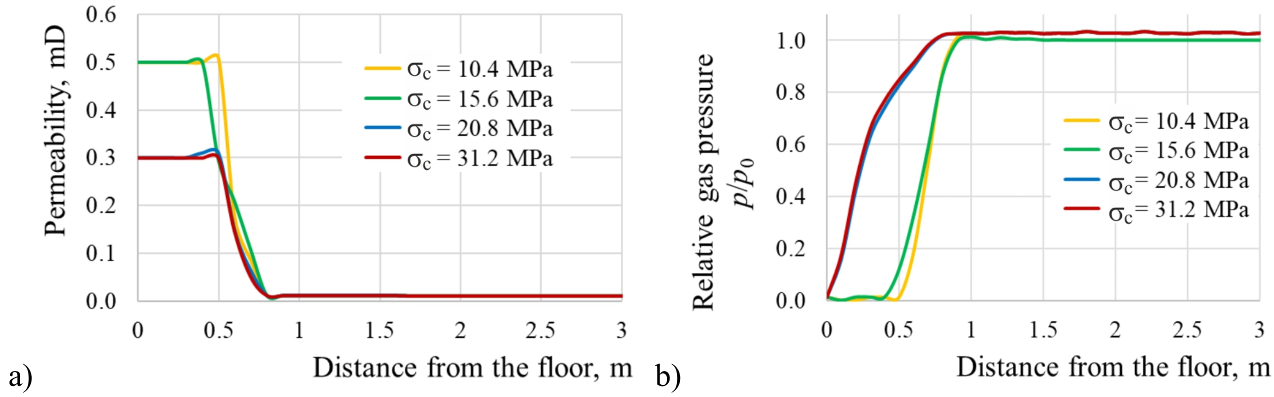

a) permeability k; b) relative gas pressure p/p_0

Figure 9 – Graphs of changes in filtration parameters in the floor of the stope when varying the siltstone's strength limit

If the stronger siltstone bed is located above the sandstone, its permeability at the time step $i = 10$ is insufficient for the development of an intensive filtration process, and in this case it is an obstacle that delays or completely prevents the degassing of gas-bearing rocks that lie below.

5. Conclusions

As shown in [1], some critical combination of stress-controlled in situ sandstone permeability and gas pressure is significant factor in rock-gas outburst occurrence. Therefore, probably, unloading of outburst-prone rocks from rock pressure and lowering formational gas pressure due to degassing contribute to reducing their outburst hazard. It should be noted that the speed of these processes should play a significant role in this.

A numerical simulation of the coupled processes of rock deformation and gas filtration was performed to study the change in the stress state and the process of methane emission from outburst-prone rocks. A stope with sections of powered support was considered, in the floor of which there are siltstone and outburst-prone sandstone. The calculations were made with variations in the thickness and strength of the siltstone bed above the sandstone.

It is shown that the values of the maximum and minimum components of the principal stress tensor gradually decrease in the floor of the stope, the sandstone is unloaded from the rock pressure. This leads to an increase in its permeability and the intensity of the methane filtration process; outburst-prone sandstone is gradually degassed, which reduces its outburst hazard.

The composition of near-contour rocks greatly affects the distribution of geomechanical and filtration parameters. If there is the siltstone bed above the sandstone, a not unloaded bridge with lower permeability appears at their contact, and degassing of the sandstone slows down significantly. If the thickness of the siltstone bed increases, the width of this bridge also increases, and methane filtration in the floor of the stope stops. The strength of the siltstone also affects the considered deformation and filtration processes, because it depends on this property whether the siltstone bed will be destroyed completely or remain intact.

The values of permeability coefficients in the floor of the stope, in siltstones with lower strength, are very high, and therefore methane freely flows from the gas-bearing sandstone into the mine atmosphere. If the stronger siltstone bed is located above the sandstone, its permeability is insufficient for the development of an intensive filtration process, and in this case it is an obstacle that delays or completely prevents the degassing of gas-bearing rocks that lie below.

The results of the above analyses should aid evaluation of potential measures to prevent the rock-gas outburst during blasting operations for the movement of sections of powered support in the stope. A better understanding of this problem could save considerable time and expense for future technological operations in similar mining conditions.

REFERENCES

1. Butt, S.D., Frempong, P.K., Mukherjee, C. and Upshall, J. (2006), "Characterization of the permeability and acoustic properties of an outburst-prone sandstone", *Journal of Applied Geophysics*, no. 58, pp. 1–12. https://doi.org/10.1016/j.jappgeo.2005.04.002

2. Aston, T., Kullmann, D. and Barron, K. (1990), "Modelling of outbursts at # 26 Colliery, Glace Bay, Nova Scotia. Part 1. Outburst history and field data", *Mining Science and Technology*, no. 11, pp. 253–260. https://doi.org/10.1016/0167-9031(90)90945-O

3. Li, X.Z. and Hua, A.Z. (2006), "Prediction and prevention of sandstone-gas outbursts in coal mines", *International Journal of Rock Mechanics and Mining Sciences*, no. 43(1), pp. 2–18. https://doi.org/10.1016/j.ijrmms.2005.03.021

4. Mineev, S.P. (2018), "Some issues on blast-free mining of prone-to-outburst rocks", *Geo-Technical Mechanics*, no. 138, pp. 37–92. https://doi.org/10.15407/geotm2018.01.037

5. Butt, S.D. (1999), "Development of an apparatus to study the gas permeability and acoustic emission characteristics of an outburst-prone sandstone as a function of stress", *International Journal of Rock Mechanics and Mining Sciences*, no. 36, pp. 1079–1085. https://doi.org/10.1016/S1365-1609(99)00067-2

6. Kullmann, D. and Barron, K. (1990), "Modelling of outbursts at 26 Colliery, Glace Bay, Nova Scotia. Part 3: Comparison of model results and field data", *Mining Science and Technology*, no. 11, pp. 269–280. https://doi.org/10.1016/0167-9031(90)90969-Y

7. Krukovska, V.V., Krukovskyi, O.P., Kocherga, V.M. and Kostrytsia, A.O. (2022), "Solving coupled problems of geomechanics and gas filtration for mining safety ensuring", *Geo-Technical Mechanics*, no. 160, pp. 106–122. https://doi.org/10.15407/geotm2022.160.106

8. Krukovskyi, O.P., Krukovska, V.V. and Kostrytsia, A.O. (2024), "Numerical study of time-dependent stresses in the floor of the stope with powered support", *IOP Conference Series: Earth and Environmental Science*, no. 1348 (1), 012030. https://doi.org/10.1088/1755-1315/1348/1/012030

9. Cheng, G. (2015), "Discussion of sandstone outburst mechanism by rock drivage in deep mine coal-bearing strata", *Advanced Materials Research*, no. 1092–1093, pp. 1388–1393. https://doi.org/10.4028/www.scientific.net/AMR.1092-1093.1388

10. Guo, C., Xian, X., Li, X., Yao, W. and Jiang, Y. (2009), "Outburst orientation of sandstone under gravitational field", *Journal of University of Science and Technology Beijing*, no. 31(12), pp. 1487–1492.

11. Baranov, V.A. (2000), Structural transformations of Donbass sandstones and forecast of their outburst hazard, D. Sc. Thesis, Geology of solid fossil fuels, M.S. Poliakov Institute of Geotechnical Mechanics of the National Academy of Sciences of Ukraine, Dnipropetrovsk, Ukraine.

12. Bezruchko, K.A. (2016), "Determination of parameters of the reservoir-screen boundary for low-porosity sandstones of the coal-bearing strata", *Coal of Ukraine*, no. 11–12, pp. 58–63.

13. Bezruchko, K.A. (2023), "The impact of moisture content on outburst hazard of sandstones in coal-bearing strata international journal of earth sciences knowledge and applications", *International Journal of Earth Sciences Knowledge and Applications*, no. 5(3), pp. 343–350. https://www.ijeska.com/index.php/ijeska/article/view/348/326

14. He, M.C., Nie, W., Zhao, Z.Y. and Guo, W. (2012), "Experimental investigation of bedding plane orientation on the rockburst behavior of sandstone", *Rock Mechanics and Rock Engineering*, no. 45, pp. 311–326. https://doi.org/10.1007/s00603-011-0213-y

15. Barron, K. and Kullmann, D. (1990), "Modelling of outbursts at # 26 Colliery, Glace Bay, Nova Scotia. Part 2: Proposed outburst mechanism and model", *Mining Science and Technology*, no. 11, pp. 261–268. https://doi.org/10.1016/0167-9031(90)90957-T

16. Shevelev, G.A. (1993), "Mechanism of development and attenuation of coal, rock and gas outbursts", *Geo-Technical Mechanics*, no. 1, pp. 46–49.

17. Bulat, A.F. and Bezruchko, K.A. (2015), *Sistema voda-gaz v massive gornyih porod Donbassa* [Water-gas system in the Donbass rock massif], Naukova dumka, Kyiv, Ukraine.

18. Li, X.Z., Zhang, D. and Hua, A.Z. (2002), "Influence of fluid pressure change on the deformation and stress state of surrounding rockmass of boreholes and caverns", *Geological Journal of China Universities*, no. 8, pp.106–112.

19. Bulat, A.F., Krukovskyi, O.P. and Krukovska, V.V. (2024), "Deformation of gas-bearing rocks and gas filtration during excavation of mine workings", *International Applied Mechanics*, no. 60(1), pp. 10–19. https://doi.org/10.1007/s10778-024-01259-9

20. Krukovska, V.V., Krukovskyi, O.P. and Demchenko, S.V. (2023), "Numerical analysis of the possibility of noxious gases infiltration into a shelter located in a gas-bearing coal-rock mass", *Geo-Technical Mechanics*, no. 166, pp. 95–108. https://doi.org/10.15407/geotm2023.166.095

21. Labuz, J.F. and Zang, A. (2012), "Mohr-Coulomb Failure Criterion", *Rock Mechanics and Rock Engineering*, no. 45, pp. 975–979. https://doi.org/10.1007/s00603-012-0281-7

22. Jiang, H. (2015), "Failure criteria for cohesive-frictional materials based on Mohr-Coulomb failure function", *International Journal for Numerical and Analytical Methods in Geomechanics*, no. 39, pp. 1471–1482. https://doi.org/10.1002/nag.2366

23. Krukovskyi, O.P., Mineev, S.P., Krukovska, V.V. and Belikov, I.B. (2021), "The influence of working seam thickness on permeability of barrier pillars near isolated fire sections", *Geo-Technical Mechanics*, no. 158, pp. 3–15. https://doi.org/10.15407/geotm2021.158.003

24. Krukovska, V.V. and Kocherga, V.M. (2022), "Influence of the method of gate road protection on the operating efficiency of methane drainage boreholes", *IOP Conference Series: Earth and Environmental Science*, no. 970, 012045. https://doi.org/10.1088/1755-1315/970/1/012045

25. Rust, W. (2012), *Non-Linear Finite Element Analysis in Structural Mechanics*, Springer, Hannover, Germany.

26. de Borst, R., Crisfield, M.A., Remmers, J.J.C. and Verhoosel, C.V. (2012), *Non-linear finite element analysis of solids and structures*, John Wiley & Sons, London, UK. https://doi.org/10.1002/9781118375938

27. Zienkiewicz, O.C., Taylor, R.L. and Zhu, J.Z. (2013), *The Finite Element Method: Its Basis and Fundamentals*, Butterworth-Heinemann, Amsterdam, Netherlands.

28. Shkuro, L.L. (2005), “Studies of basic indexes collector properties, which to influence on methanogenetic sandstones”, *Geo-Technical Mechanics*, no. 59, pp. 170–175. http://dspace.nbuv.gov.ua/handle/123456789/141314

29. Lukinov, V.V., Toropchyn, O.S., Hunia, D.P., Kaplanets, M.E. and Radovanov, S.V. (2005), “Problems of superficial degassing on the coal deposits”, *Geo-Technical Mechanics*, no. 53, pp. 138–143.

About the authors

Krukovska Viktoriia, Doctor of Technical Sciences (D.Sc.), Senior Researcher, Senior Researcher in Department of Dynamic Manifestations of Rock Pressure, M.S. Poliakov Institute of Geotechnical Mechanics of the National Academy of Sciences of Ukraine (IGTM of the NAS of Ukraine), Dnipro, Ukraine, vikakrukk@gmail.com, ORCID ***0000-0002-7817-4022.***

Krukovskyi Oleksandr, Corresponding Member of NAS of Ukraine, Doctor of Technical Sciences (D.Sc.), Deputy Director of the Institute, M.S. Poliakov Institute of Geotechnical Mechanics of the National Academy of Sciences of Ukraine (IGTM of the NAS of Ukraine), Dnipro, Ukraine, igtm@ukr.net, ORCID ***0000-0002-2659-5095.***

Yanzhula Oleksii, Candidate of Technical Sciences (Ph.D.), Director for Technical Development and Investments, Coal Directorate METINVEST HOLDING LLC, Pokrovsk, Ukraine, aleksey.yanzhula@metinvestholding.com, ORCID ***0009-0000-8906-0656.***

Kostrytsia Andrii, Postgraduate Student, M.S. Poliakov Institute of Geotechnical Mechanics of the National Academy of Sciences of Ukraine (IGTM of the NAS of Ukraine), Dnipro, Ukraine, igtm.sektor@gmail.com.

Kocherga Viktor, Candidate of Technical Sciences (Ph. D), Chief Technologist in Department of Pressure Dynamics Control in Rocks, M.S. Poliakov Institute of Geotechnical Mechanics of the National Academy of Sciences of Ukraine (IGTM of the NAS of Ukraine), Dnipro, Ukraine, kocherga.v.n@gmail.com

ВПЛИВ ОСОБЛИВОСТЕЙ РОЗТАШУВАННЯ ВИКИДОНЕБЕЗПЕЧНИХ ПОРІД В ПІДОШВІ ОЧИСНОЇ ВИРОБКИ НА РОЗПОДІЛ ПОЛЯ НАПРУЖЕНЬ І ПРОЦЕС ЇХ ДЕГАЗАЦІЇ

Круковська В., Круковський О., Янжула О., Кострица А., Кочерга В.

Анотація. Викиди породи і газу відбуваються, коли гірничі виробки проводяться поблизу пісковиків із низькою проникністю, які містять газ під високим тиском, і більшість з них спричинені проведенням буро-підривних робіт. Зокрема, при затисканні в лаві секцій механізованого кріплення під ним необхідно підривати породу, що є небезпечним, якщо в підошві очисної виробки розташований викидонебезпечний пісковик. Одним із факторів виникнення викиду породи і газу є певна комбінація залежної від напруження проникності пісковика і приконтурних порід і тиску газу. Тому метою роботи є дослідження зміни напруженого стану вміщуючих порід і процесу фільтрації газу у викидонебезпечному пісковику, розташованому в підошві очисної виробки, при різному складі приконтурних порід. Для досягнення мети використовувались методи чисельного моделювання залежних від часу зв’язаних процесів пружно-пластичного деформування і фільтрації газу. Розглянуто очисну виробку з секціями механізованого кріплення, в підошві якої залягають алевроліт і викидонебезпечний пісковик. Розрахунки виконано із варіюванням потужності і міцності шару алевроліту над пісковиком.

Показано, що в підошві виробки значення максимальної і мінімальної компонент тензора головних напружень поступово знижуються, пісковик розвантажується від гірського тиску. Це призводить до зростання його проникності, початку фільтрації метану і процесу дегазації. Склад приконтурних порід в підошві очисної виробки дуже впливає на розподіл геомеханічних і фільтраційних параметрів. За наявності шару алевроліту з певною міцністю над пісковиком з’являється нерозвантажена перемичка з меншою проникністю і дегазація пісковику значно уповільнюється. При зростанні потужності алевроліту ширина цієї перемички зростає, фільтрація метану в підошві виробки припиняється. В цьому випадку він є перешкодою, яка затримує або повністю попереджає дегазацію газоносних порід, які лежать нижче.

Результати наведеного аналізу повинні допомогти в оцінці потенційних заходів для попередження викидів пісковика і газу під час виконання буро-підривних робіт для пересування секцій механізованого кріплення в очисній виробці. Краще розуміння цієї проблеми може заощадити значний час і кошти для майбутніх технологічних операцій в аналогічних гірничотехнічних умовах.

Ключові слова: викид породи і газу, деформування порід, зв’язані процеси, очисна виробка, фільтрація метану, чисельне моделювання.